

# Overview of helical foil winding design for planar inductors

## Part 2: DC-Filter Inductors

D C Pentz

Group on Electronic Energy Processing  
University of Johannesburg  
Johannesburg, South Africa  
davidp@uj.ac.za

**Abstract**— This paper further elaborates on the topic of conductor optimization for planar helical foil windings. Part 1 of this work briefly covers the classical design methods and new schemes suggested for ac-inductors supported by two case studies. Optimisation of the windings used in filter inductors, carrying both ac- and dc-currents simultaneously, are handled in Part 2 of the publication. Winding shaping techniques, formerly used for cylindrical conductor windings, are adapted for helical foil windings placed in gapped cores. The concept of varying conductor thickness is further used here to achieve substantial reduction in overall losses with the further advantage of drastically reducing the time needed for obtaining the optimal winding shape. The calorimetric methods used to verify results experimentally are also included in this part.

**Index Terms**— Planar component, planar winding, transformer, inductor, helical winding, shaped winding.

### I. INTRODUCTION

In inductors with a concentrated air gap in the magnetic material, the fringing flux of the air gap will couple with the conductors close to the air gap and the eddy currents induced in the conductors will result in a loss component which is measurable through the winding resistance. The cylindrical wire winding notching techniques in the region of an air gap, first suggested by Sinclair [1] and later used by Sullivan et al. [2], is adopted for the helical foil wound structures in this work. Experimental windings are designed using the methods suggested in Part 1 of this publication as well as the new method introduced in [3]. This method greatly reduces the time required to complete the optimisation process because it does not require FEM-simulations to be performed. Detail on the FEM-simulations, experimental methods and converters used may be found in [3]. Calorimetric methods used in [3] are discussed in more detail.

### II. SHAPED HELICAL PLANAR WINDING

Figure 1 illustrates how the foil conductors, of a helical inductor winding, are shaped in the region of the air gap. More

shaping techniques are summarised in [3]. Semi-circular notches are used as suggested in [2]. The edges of the conductors are moved further from the air gap and the reduced flux density reduces the induced loss component. The fact that the width of the foil conductor is reduced in the process, however, means that the DC-resistance increases as indicated in Fig. 2.

FEM simulations have to be used to find the optimal notch radius,  $r_{opt}$ , and proves to be a very time consuming process since the new winding configuration around the air gap has to be redrawn several times to find the general region of the minimum loss point and then several more simulations have to be performed to accurately pinpoint the position of minimum loss. It should also be noted that for non-sinusoidal current excitation the FEM-simulations are performed on the fundamental waveform as well as all the significant harmonic components to find the conductor losses through superposition. More detail on the simulation process may be found in [3]. A MATLAB-implementable algorithm for fast loss predictions was developed and tested for arbitrary waveforms [4] and [5] but will not be discussed further in this paper. The loss reduction values achieved using shaping techniques depend on the harmonic content of the ripple component of the current. The combined case study done in [3] is discussed in the next section. Up to this point the Hurley and Perry methods discussed in Part 1 of this publication are used to design the

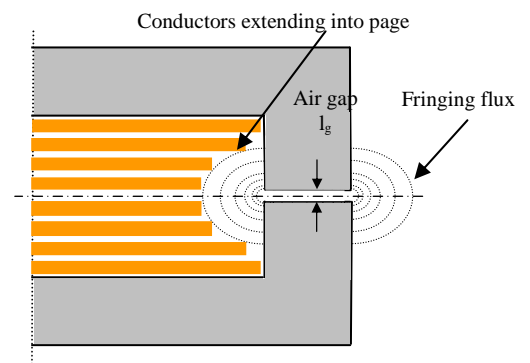


Fig. 1. Winding shaped in air gap region

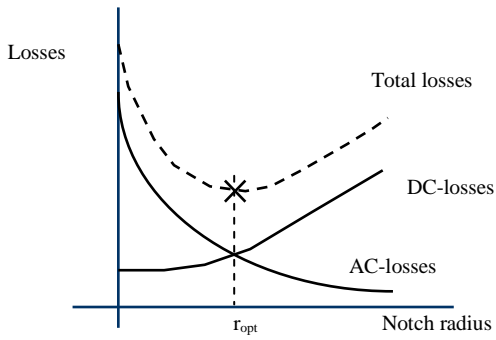


Fig. 2. Ac- and dc-losses as a function of notch radius

desired conductor thickness for each layer in the winding section and only then is the winding notched. This results in a reduction in the ac-losses function of the increased notch radius while the dc-resistance increases at the same time.

### III. PROPOSED SOLUTION – NOTCHING METHOD WITH MAINTAINED DC-RESISTANCE

In the combined case study a considerable ac-ripple is superimposed on a dc-current. Conductors in the winding section are optimised for a 100kHz current waveform with an average value of 8A and a ripple ratio of 50%, using the Hurley method, i.e. all the conductors are initially of the same dimensions. The notching process is now started. It is now suggested that the increase in the dc-resistance, previously caused by the reduction in the conductor width, is counteracted by increasing the thickness of this particular layer [3],[4]. Figures 3 and 4 show the effect graphically. The resulting winding is similar in appearance with the thicker conductors toward the centre of the winding, where the MMF is also at a minimum. The winding thickness increases by approximately 10% in this case. Not only is the performance slightly superior, but the time required to get to an optimal solution is greatly reduced. It should again be emphasised that the increase in winding thickness should be kept in mind from the start of the design process, because the maximum notch radius is effectively limited by the initial available headroom in the window of the magnetic core.

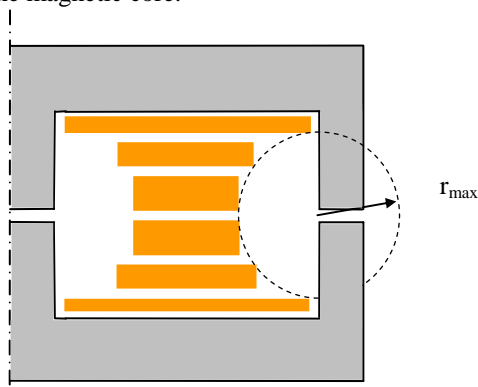


Fig.3. Shaped winding with layers of equal dc-resistance

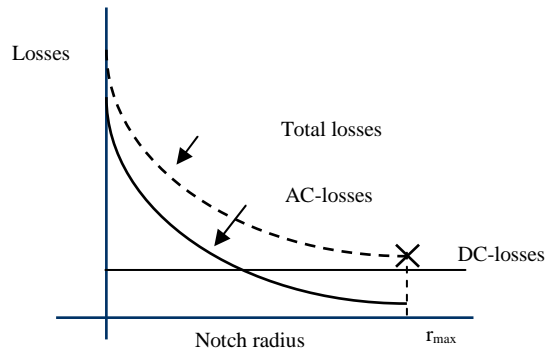


Fig. 4. AC- and DC-losses

### IV. EXPERIMENTAL RESULTS

A case study reported in [3] shows a result where three of four possible windings are designed and constructed for the waveform shown in Fig. 5. The reference winding (L1) winding is optimised using the Hurley method resulting in all the layers being constructed with the same thickness material. This winding is not shaped in the air gap region. A second winding (L2) is initially optimised the same as L1 after which it is then shaped to the optimum notch radius around the air gap determined through a process of performing several FEM-simulations as illustrated in Fig. 2. The third winding (L3) is designed using the Hurley-method to start with and then notched to the optimum radius. The method, where the dc-resistance is kept constant while increasing the notch radius to the maximum value permitted by the winding window, is now applied to the last winding constructed (L4) after starting out in the same way as L1 and L2 [3]. It should again be noted that the time to complete the optimization process is reduced significantly. The L3-winding was ultimately not constructed. The optimization process for L4 actually requires no FEM-simulation, yet it is still performed to obtain a loss improvement value that may be of use as a benchmark for the experimental results and shown in Fig. 6 with the other FEM-predictions and the respective relative improvements in winding losses. Photographs of the physical windings are

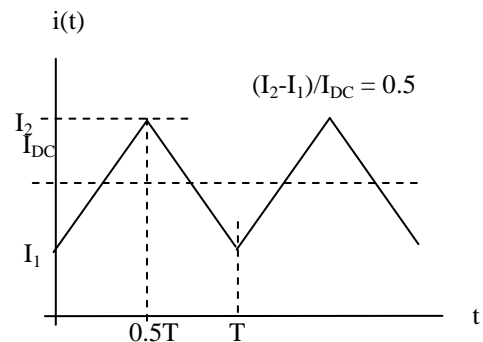


Fig. 5. Current waveform

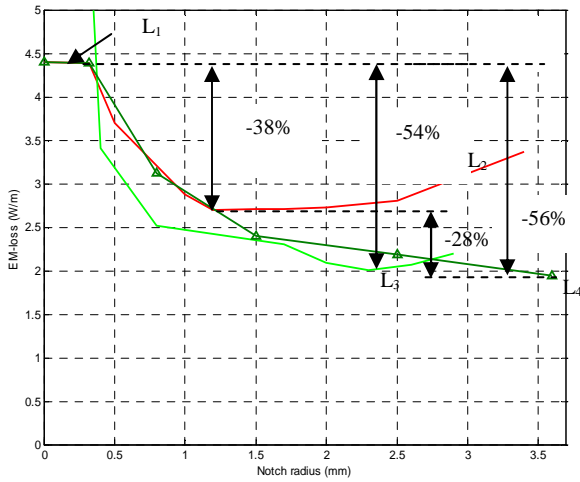


Fig. 6. FEM loss predictions for shaped windings

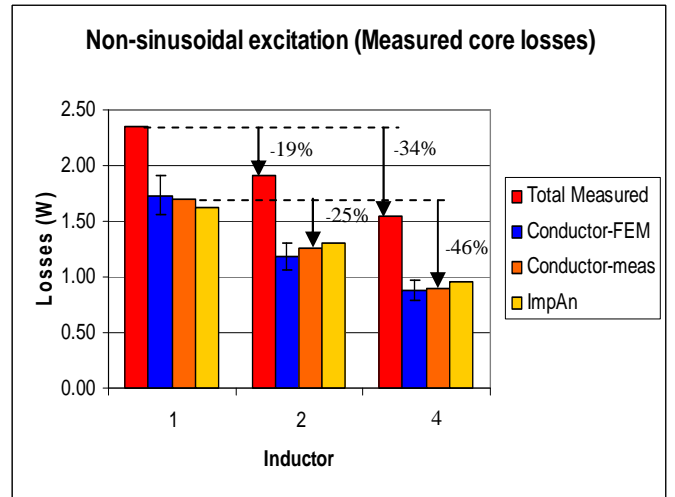


Fig. 8. Comparative calorimetric results for full-load non-sinusoidal excitation

shown in Fig. 7. The measured results are all shown graphically in Fig. 8. Results were confirmed using calorimetric methods of loss measurement, which is discussed in the next section.

Core loss estimation for this experiment requires much more attention than for cases where the core excitation is sinusoidal.

First of all the non-linear nature of the core material deems the Fourier approach invalid. Methods proposed in [6] and [7] and used in some of the case studies in [3] may be used to estimate core losses for non-sinusoidal excitation with no dc-offset. However, the waveform presented in Fig. 5 contains harmonics as well as a dc-component. It is shown in [8] that the ac-exursion in the flux density around a dc-offset causes core losses which by far exceeds values obtained by the same ac-exursion around the origin on the BH-curve. For this reason a simplified experiment was set up to measure the core losses for the case study at hand. The strategy implemented included the reduction of the amount of conductor material

whilst maintaining the same ac- and dc-flux in the core [4]. This is made possible by removing the air gap. A single turn cylindrical conductor winding centred in the window is used for this purpose. The winding, which does not experience air gap proximity loss, can be characterised accurately through measurement with an LCR-meter and confirmed with a FEM-simulation. The core losses are then measured using the calorimetric method discussed in the next section and subtracted from the total losses to evaluate the performance of the winding. This result is also included in Fig. 8. The conductor loss improvements obtained through measurement are lower than predicted with FEM but the general trends are notable. Differences may be attributed to a number of factors including general measurement error, error in measuring the core losses and the fact that winding overhang is treated the same as the parts embedded in the core. Physical tolerances of the cores also have a large effect on the measured values because small variations in the distance between the winding and the air gap affect the coupling with the fringing flux. The effect of the winding shape on the inductance is also shown and discussed in [3].

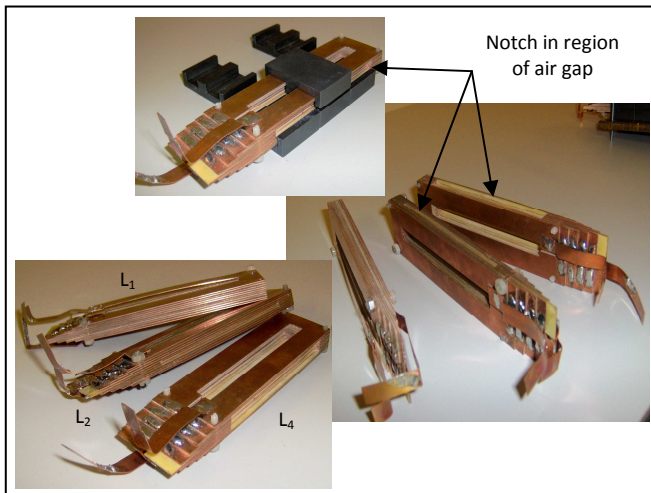


Fig. 7. Photographs of the three test inductors

## V. CALORIMETRIC MEASUREMENT METHOD

Experimental verification of the various results is also an aspect that received much attention during this study [4]. Loss measurement through electric measurements in high frequency converters has always been very difficult due to the relatively low active power component buried in the reactive power. Calorimetric methods were thus used throughout the study. Methods discussed in [9] and [10] are used and variations are made for the purpose of this study. The basic principle of calorimetric measurement, governed by  $E = mc\Delta t$ , is applied where  $E$  is the energy required to raise the temperature of a mass  $m$ , with specific heat capacity  $c$ , by an amount of  $\Delta t$  degrees Celcius. The device under test (DUT) and a power resistor is mounted on a heat sink, which is again mounted in a thermally insulated container. Thermal insulating material is

used to fill up all the space that will otherwise be filled with air to prevent the air from moving. This container is shown in the photograph in Fig. 9 without the material that fills up the cavities. This container is then placed in an incubator. The characterization procedure is as follows. A known amount of power is dissipated in the resistor by simply connecting it to a dc-power supply and appropriate measurement instrumentation. The temperature inside the container will increase as a function of time. The incubator temperature is set to track the temperature in the container. This way the temperature gradient is cancelled and thermal energy is not likely to “leak” through the walls of the container. Figure 10 shows the increase in temperature with and without the thermal tracking strategy. The increase in temperature is linear, as expected, if the thermal barrier is set up. The leakage effect is however noticeable if the incubator temperature is kept constant at a value lower than the heat sink temperature. In [10] heating plates, surrounding the device under test, are used to cancel thermal gradients across the walls of the container.

The theoretical increase in temperature as a function of time in Fig. 10 is determined by weighing the various components, using the respective c-values of the materials and determining the rate at which the temperature should increase. From the measured results an equivalent mc-product is determined for the device under test, the high power resistor, the heat sink they are mounted on as well as the surrounding thermal insulation material and the trapped air in the container made of polystyrene. This mc-product is in all likelihood more accurate than the theoretical value, which does not include the trapped air and the thermal insulation material into account.

The performance of this calorimeter is easily evaluated and the calibration refined by using a number of data sets [4]. Error margins of  $\pm 5\%$  could be maintained throughout the process. The methods could further be improved if instrumentation less susceptible to the converter noise is used. During the experimental procedure the converters had to be switched off momentarily to obtain the correct temperature reading .

## VI. CONCLUSION

This paper follows on Part 1, which covers various aspects of the optimisation of helical, foil wound planar windings.

Part 2 covers the aspect of optimising the conductor

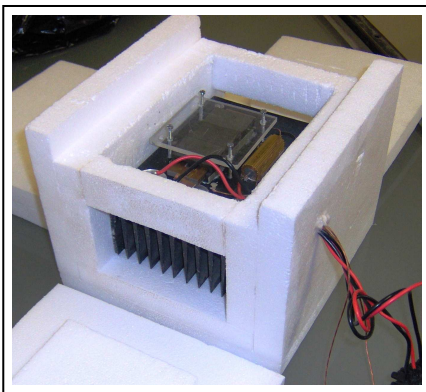


Fig. 9. Photograph of proposed calorimeter

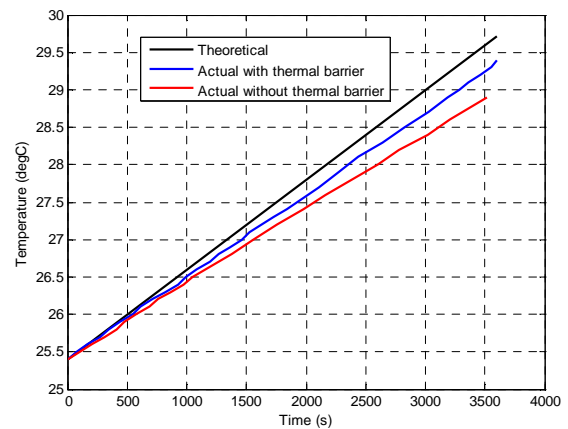


Fig. 10. Initial thermal experiment

thickness and the shape of the notch around the core gaps. The method proposed for optimisation of filter inductor windings brings about a reduction in the losses, in the order of 46% in this case, while drastically reducing the time of the optimisation process and eliminating the need for FEM-simulations. Planar helical foil windings for the ideal platform for implementation of winding shaping techniques because high levels of precision are obtainable during manufacturing. The calorimetric methods used to experimentally verify the results, predicted using FEM-simulations, are also covered and evaluated.

## REFERENCES

- [1] A. Sinclair, J.A. Ferreira, “Optimum Shape for AC foil Conductors.”, *IEEE Power Electronics Specialists Conference (PESC)*, vol. 2, June 1995.
- [2] J.D. Pollock, C.R. Sullivan, “Modelling Foil Winding Configurations with Low AC and DC Resistance.”, *IEEE Power Electronics Specialists Conference (PESC)*, 2005.
- [3] D.C. Pentz, I.W. Hofsaier, “A Performance Evaluation of Shaped Planar Inductor Windings in Gapped Core Applications Utilizing Turns With Constant DC-Resistance.”, *IEEE Power Engineering Society Conference and Exposition in Africa*, 2007, Power Africa '07, 16-20 July 2007.
- [4] D.C. Pentz, “Aspects of Conductor Optimization for High-Frequency Helical Foil Wound Planar Inductors.”, Thesis, University of Johannesburg, 2008.
- [5] D.C. Pentz, I.W. Hofsaier, “Novel Technique for Shaped Planar Inductor Winding Optimization in Gapped Core Applications.”, *IEEE Power Engineering Society Conference and Exposition in Africa*, 2007, Power Africa '07, 16-20 July 2007.
- [6] K. Venkatachalam, C.R. Sullivan, T. Abdhullah, H. Tacca, “Accurate Prediction of Ferrite Core Loss with Non-Sinusoidal Waveforms Using Only Steinmetz Parameters.”, *8<sup>th</sup> IEEE Workshop on Computers in Power Electronics, COMPEL 2002*.
- [7] W. Shen, “Design of High-Density Transformers for High-Frequency High-Power Converters.”, Dissertation, Virginia Polytechnic Institute and State University, Blacksburg, Virginia, July 2006.
- [8] C.A. Baguley, B. Carsten and U.K. Madawala, “The Effect of DC Bias Conditions on Ferrite Core Losses.”, *IEEE Transactions on Magnetics*, vol. 44, no. 2, Feb. 2008.

- [9] Chucheng Xiao, Gang Chen and Willem G.H. Odendaal, "Overview of Power Loss Measurement Techniques in Power Electronic Systems.", IEEE Transactions in Industry Applications, vol. 43, no. 3, May/June 2007.
- [10] Gang Chen, Chuchen Xiao and W.G. Odendaal, "An Apparatus for Loss Measurement of Integrated Power Electronic Modules: Design and Analysis.", Conference Record of the Industry Applications Conference, 37<sup>th</sup> IAS Annual Meeting..